REPORT DOCUMENTATION PAGE

AFRL-SR-BL-TR-01-

0512

1. AGENCY USE ONLY (Leave Blank)	2. REPORT DATE Final	3. REPORT TYPE AND DATES COVERED 1 Feb 1998 - 30 Nov 2000

4. TITLE AND SUBTITLE Optical Supramolecules for Chemical & Physical Sensing	5. FUNDING NUMBERS F49620-98-1-0203 5303 - BV 61102F

6. AUTHORS
Daniel G. Nocera

7. PERFORMING ORGANIZATION NAME(S) AND ADDRESS(ES) Massachusetts Institute of Technology Department of Chemistry 77 Massachusetts Avenue Cambridge MA 02139	8. PERFORMING ORGANIZATION REPORT NUMBER

9. SPONSORING / MONITORING AGENCY NAME(S) AND ADDRESS(ES) Lt. Col. Paul C. Trulove, Ph.D. AFOSR/NL 801 North Randolph Street, Room 732 Arlington VA 22203-1977	10. SPONSORING / MONITORING AGENCY REPORT NUMBER

11. SUPPLEMENTARY NOTES

12a. DISTRIBUTION / AVAILABILITY STATEMENT

12b. DISTRIBUTION CODE

13. ABSTRACT (Maximum 200 words)

Proposal F49620-98-1-0203 addresses the diverse chemical and physical sensing needs of the United States Air Force. All the techniques developed in this program are based on monitoring a bright luminescence from a molecule or supramolecule reporter site. By controlling the rates for energy flow within the supra/molecular architecture, the intensity and lifetime of the luminescence may be adjusted to address chemosensing and physical sensing applications of interest to the Air Force. Sub-projects within F49620-98-1-0203 included he development of an optical chemosensor for the detection of polyaromatic signatures of JP4, and the development of new optical diagnostic techniques to measure vorticity and pressure over aerodynamic surfaces.

20011012 033

14. SUBJECT TERMS chemosensors, luminescence, pressure sensitive paints, temperature sensitive paints, optical diagnostics molecular tagging velocimetry, rotating airfoil, microfluidics	15. NUMBER OF PAGES 17
	16. PRICE CODE

17. SECURITY CLASSIFICATION OF REPORT UNCLASSIFIED	18. SECURITY CLASSIFICATION OF THIS PAGE UNCLASSIFIED	19. SECURITY CLASSIFICATION OF ABSTRACT UNCLASSIFIED	20. LIMITATION OF ABSTRACT SAR

Table of Contents

1. Abstract

Proposal F49620-98-1-0203 addresses the diverse chemical and physical sensing needs of the United States Air Force. All the techniques developed in this program are based on monitoring a bright luminescence from a molecule or supramolecule reporter site. By controlling the rates for energy flow within the supra/molecular architecture, the intensity and lifetime of the luminescence may be adjusted to address chemosensing and physical sensing applications of interest to the Air Force. Sub-projects within F49620-98-1-0203 included he development of an optical chemosensor for the detection of polyaromatic signatures of JP4, and the development of new optical diagnostic techniques to measure vorticity and pressure over aerodynamic surfaces.

2. Technical Summary of Work Accomplished

We seek to address the diverse chemical and physical sensing needs of the United States Air Force. All the sensing techniques developed in this program are based on monitoring a bright luminescence from a probe molecule, supramolecule or material. We define the fundamental parameters that control the nonradiative and radiative energy flows to allow us to tailor the luminescence intensity and lifetime of the probe for the specific Air Force sensing application. Application areas that this research program was concerned with over the past funding cycle were: (1) the development of chemosensors for the detection and monitoring of mono- and bicyclic aromatics in jet fuel; (2) the development of new pressure sensitive paints to sense pressure over aerodynamic surfaces that are under investigation in the subsonic wind tunnel testing facility at Wright Patterson Air Force Base (Experimental Operations and Diagnostics Branch of the Aeromechanics Division of the Flight Dynamics Directorate); and (3) and the elaboration of the optical diagnostics technique that we invented to physically sense flows over airfoils. Our results obtained in each of these areas is now described.

2.1. Chemosensing

Our chemosensing efforts have revolved around the detection of the chemical signatures of jet fuels for field monitoring and environmental remediation at United States Air Force bases and storage facilities. The fuel standard for the Air Force is JP4/8, which has appreciable mono- and bicyclic aromatic hydrocarbon content. Prior to our work, most optical detection methods of aromatics and polyaromatics relied on measuring the fluorescence of these constituents by direct excitation and detection [1]. Practically, direct laser-induced fluorescence approaches are problematic because the blue fluorescence of the analyte must be deconvoluted from the blue fluorescence of other organic interferents. An alternative transduction scheme relies on the displacement of fluorophores from DNA by large polycyclic aromatic hydrocarbons [2]. But the low affinity of small cyclic aromatics for DNA has prevented their detection by this method.

2.1.1. The Signal Transduction Mechanism of an Optical Chemosensor for Aromatic Hydrocarbons

Our approach to detect aromatic hydrocarbons was based on designing a chemosensor [3,4] that operated by the "3R scheme"- recognize, relay and report - shown in Figure 1 [2.4.1]. A non-covalent molecular recognition event at the receptor site is communicated, by physical or chemical means, to a reporter site, which produces a measurable signal. A rapid equilibrium between the analyte and receptor site affords the chemosensor a real-time response that varies with the concentration of analyte.

In our design of Figure 1, we sought chemosensors that would operate in an aqueous environment. Accordingly, we chose the miniature bucket of a cyclodextrin (CD) as the receptor site. Hydroxyl groups of the D-glucose subunits composing the CD impart water solubility to the bucket whereas the hydrocarbon rings of the D-glucose subunits define a hydrophobic interior suitable for binding guests. Thus a CD bucket will dissolve in water but will fill itself with aromatic guests [5,6]. Binding selectivity (and therefore selectivity in chemosensor function) for mono- and bicyclic aromatics is conveniently

Figure 1. The 3R scheme used for chemosensor development. A = aromatic analyte.

achieved with the cavity size of the bucket. β-CD (7 D-glucose rings composing the bucket) will bind BTEXs (benzene, toluene, ethylbenzene, xylene) and bicyclic aromatics (e.g., naphthalene, biphenyl) but not larger polyaromatics. Because we were interested in total aromatic content, β-CD proved to be the ideal receptor site for our targeted chemosensing application.

The creation of a chemosensor required us to modify the β-CD receptor site for signal generation. In our construct, the hydroxyl functionality at the rim of the bucket offered sites to attach a discrete reporter site. Here, our requirement for signal transduction was a luminescent optical signal owing to its sensitivity and ease of implementation [7,8]. With regard to the 3R scheme of Figure 1, luminescence-based signaling offers another significant advantage. A sound knowledge of the photophysical properties that govern a particular luminescence event enabled us to facilely tailor the signal transduction mechanism.

The final requirement we imposed on our chemosensor design was that a luminescence signal be *triggered* upon recognition of the analyte in the CD bucket. This is in contrast to typical luminescence signal transduction schemes, which generally rely on the detection of a quenched luminescence signal. Although easy to implement, quenching-based schemes are intrinsically limited. Electronic excited states are not very discriminating and are susceptible to any number of quenching processes, causing quenching-based chemosensors to be prone to interferents. Additionally, a detection signal produced by quenching complicates chemosensor design because the decrease in luminescence intensity must be measured against a bright background. As we have stressed, the drawbacks of quenching-based detection are overcome when an analyte triggers a luminescence signal relative to a dark background. Thus we sought to build a chemosensor that produced a luminescence signal when the CD bucket was filled with an aromatic hydrocarbon.

An extensive study [2.4.2 and 2.4.3] allowed us to meet the above design criteria and led to the creation of 1. A diethylenetriaminepentaacetic acid (DTPA) macrocycle was tethered via both of its nitrogens to the primary rim of the CD, allowing for a Tb^{3+} ion to be cradled below
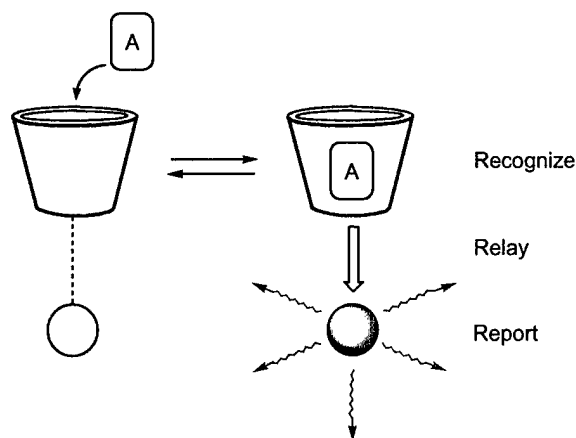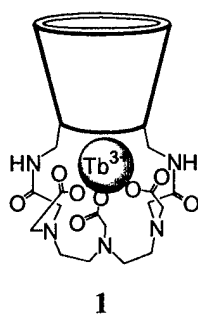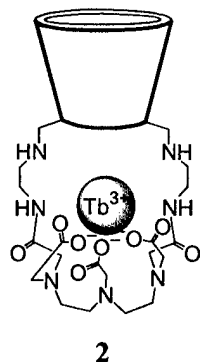
3

the bucket [9]. In previous sensor constructs, the presence of cationic charge at the bottom of the CD undermined the hydrophobicity of the receptor site and decreased association of hydrophobic aromatics to the CD bucket was observed [10]. This diminished association of aromatics to the CD limited the overall optical response from the chemosensor. With the charge of the +3 charge of the ion reporter site neutralized by the –3 charge of the DTPA strap, aromatics enter the CD bucket of 1 with high association constants.

1

Faithful to our intended goals, a bright green luminescence is triggered upon the introduction of aromatic hydrocarbons to aqueous solutions of 1. The signal intensity increases monotonically with the concentration of aromatic hydrocarbon, reaching an asymptotic limit that was specific to the analyte. For instance, a 10% intensity enhancement was observed for 200 ppm of benzene as compared to ~4000% intensity enhancement for 10 ppm of biphenyl. The differing sensitivities of 1 to aromatics directly related to the stability constant of the 1•aromatic complex and the absorption cross-section of the aromatic. The presence of an absorption-energy transfer-emission (AETE) relay mechanism was established by examining the emission characteristics of the assembly as excitation wavelength of light is scanned. The intensity of the green luminescence from Tb^{3+} ion tracked the absorption profile of the aromatic and not that of the ion. This result unequivocally established that excitation of the Tb^{3+} ion emission was excited by light passing through the aromatic analyte.

During the past grant period, we thoroughly investigated the AETE relay mechanism by using time-resolved spectroscopy [2.4.4]. The excitation energy captured by biphenyl included in 1 was observed to appear at the $^5D_4$ state of Tb^{3+} in 12 µs. The green luminescence of the Tb^{3+} ion subsequently decayed with a lifetime of 1.6 ms. Further insight into the photophysics of the relay mechanism was provided by replacing Tb^{3+} of 1 with Gd^{3+} (which we designate as $1(Gd^{3+})$). Because Gd^{3+} excited states are too high in energy, the $1(Gd^{3+})$ complex provided a reference for the supramolecule photophysics in the absence of energy transfer to the lanthanide (Ln^{3+}) ion. A comparison of the luminescence decay kinetics for biphenyl associated to $1(Tb^{3+})$ and $1(Gd^{3+})$ leads to the model depicted in Figure 2. The AETE process is initiated by the absorption of an incident photon to produce the $^1\pi\pi^*$ excited state of biphenyl. The lanthanide facilitates intersystem crossing to the triplet from which energy transfer occurs to produce the $^5D_4$ excited state of the Tb^{3+} ion. Negligible spectral overlap precludes energy transfer by a Förster mechanism. Calculations based on the prevailing Dexter mechanism yield a donor(biphenyl)-acceptor(Tb^{3+}) distance of ~5 Å. This result is consistent with the distance measured from energy minimized molecular models of the $1(Tb^{3+})$•biphenyl complex. To further establish the role of Dexter energy transfer, our recent preparation of 2 has allowed us to systematically increase the distance between the analyte and Tb^{3+} reporter site [2.4.5]. A Dexter treatment of time-resolved energy transfer kinetics data predicts the donor-acceptor
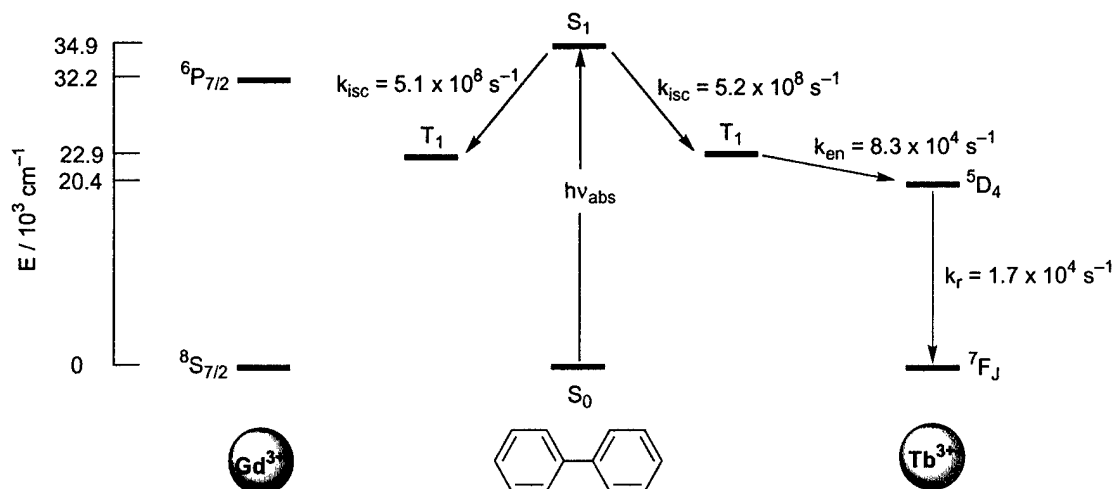
2

Figure 2. Photophysics scheme with measured rate constants for the AETE process of the binary complex formed between $1(Tb^{3+})$ and $1(Gd^{3+})$ with biphenyl.

distance in **2** to increase by ~2 Å, a distance that is in agreement with distance measurements made from energy minimized molecular modeling calculations.

In the photophysical scheme of Figure 2, the *triplet* excited state represents a staging area for energy transfer. This has also been observed for the AETE processes between triplet excited state donors and (Tb^{3+}, Eu^{3+}) complexes of modified calix[4]arenes [*11-13*]. These results, taken together with the systems described here, serve to emphasize the role of the Ln^{3+} ion to open a conduit for energy flow in supramolecular assemblies. In addition to the obvious importance of the Ln^{3+} ion as the emitting center in the AETE process, the Ln^{3+} ion also provides a mechanism to produce a long-lived donor excited state from which energy transfer may occur. In the absence of this heavy atom, the singlet-excited state of the aromatic would return to its ground state before energy transfer could occur. By channeling the singlet to a long-lived triplet, ample time is provided for the slower energy transfer process to effectively compete with the fast natural radiative and nonradiative processes of the analyte. As described below, we will take advantage of this property in our design of sensory polymers based on **1**.

2.1.2. Optical Chemosensing Thin Films for Microfluidic Platforms

A goal of our planned research is to integrate optical supramolecular chemosensors such as **1** onto microfluidic platforms (see Section 3.2.1.2). The realization of microfluidic optical chemosensors demands that the supramolecular architecture be incorporated into a matrix that is compatible with lithographic patterning protocols. Accordingly, a second major thrust of our work in chemosensing during the past funding cycle has been to develop methods to permit the attachment of the CD chemosensor onto inorganic and organic polymer host matrices.

We successfully incorporated **1** into organic host matrices by utilizing site-directed functionalization techniques. The following strategy allowed us to selectively introduce a vinyl acrylate group under mild conditions onto the secondary rim (top) of the CD bucket,

5

Scheme 1
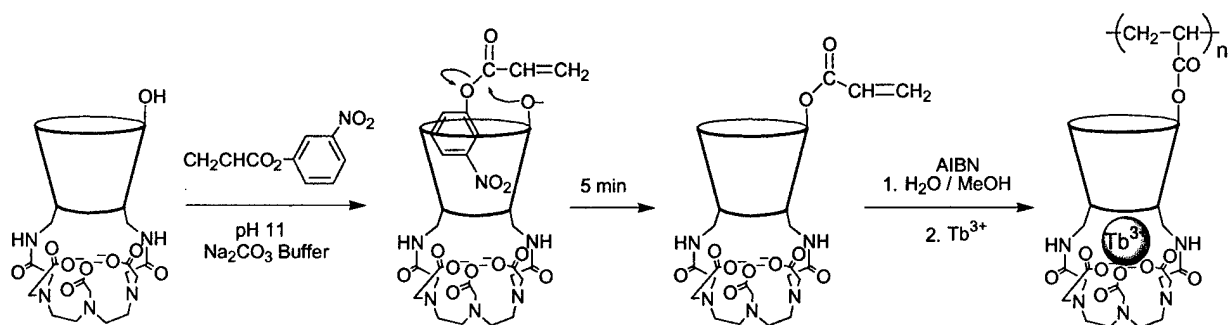
The key to the protocol was to direct site derivatization by inclusion of the polymer precursor, *m*-nitrophenyl acrylate, within the CD bucket. Polymerization of the vinyl acrylate group was induced with 2,2′-azobis(isobutyronitrile).

With the polymerization methodology established, we turned our attention to anchoring the polymer film to a substrate that was suitable for microfluidic device fabrication. 1-cm^2 square patterns of vinyl functional groups on silica slides were reacted with the vinyl acrylate modified CD as follows,

Scheme 2
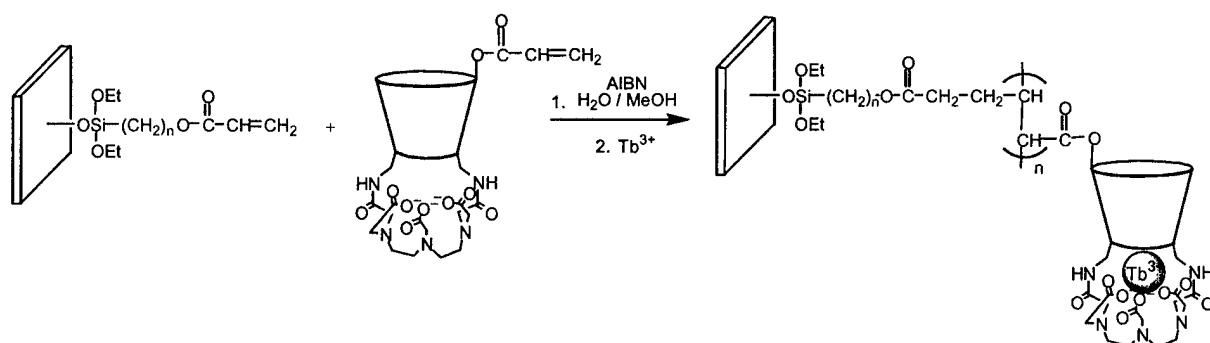
Alternatively, we found that our site-directed functionalization technique could be exploited by attaching *m*-nitrophenyl acrylate to a siloxane polymer in dry toluene using H_2PtCl_6 as a catalyst (Scheme 3). Addition of the CD chemosensor to functionalized siloxane polymer, attached to substrate, leads to coupling of the CD onto the polymer backbone. The progress of the polymerization was visually monitored with the appearance of the bright yellow color of nitrophenolate at the patterned siloxane squares. Although this procedure consistently afforded polymer films of the chemosensor attached to glass substrates, only low surface coverages.

6
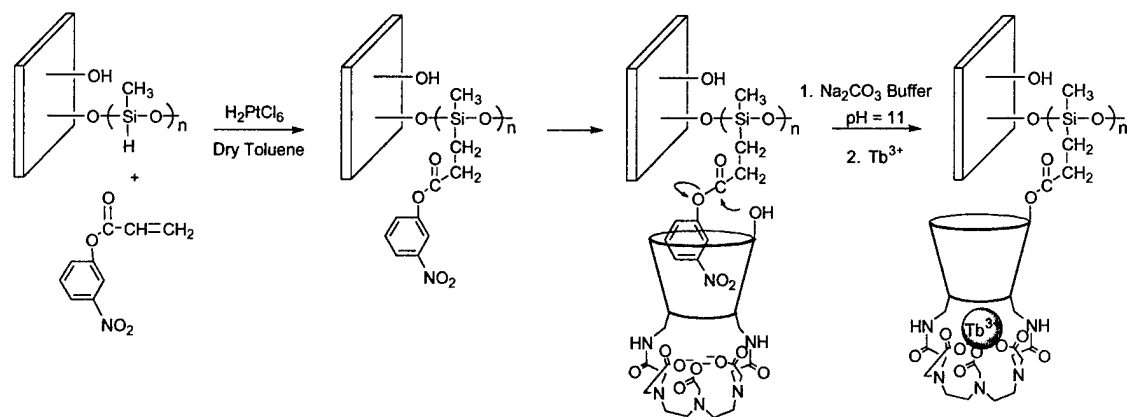
Scheme 3

       With the goal of increasing surface coverage, sol-gel polymers of **1** were prepared by the method of Scheme 4. The CD was condensed into a partially hydrolyzed tetraethylorthosilicate solution in ethanol (acid catalyzed conditions). This solution was easily spin-cast onto clean, dry, quartz substrate to give gel films of thicknesses ranging from 0.2 - 0.6 μm, which were determined by profilometry measurements. Figure 3 shows that these films provide a superb optical response to aromatics. Addition of μM concentrations of biphenyl triggers an x45 enhancement of the Tb^{3+} luminescence intensity. The enhancement proves to be concentration-dependent and is reversed by rinsing the substrate with alcohol to remove the biphenyl from the cyclodextrin cavity. Time-resolved kinetics measurements on the sol-gel thin films establish that the same AETE mechanism observed in solution prevails in the film. The decay of the biphenyl
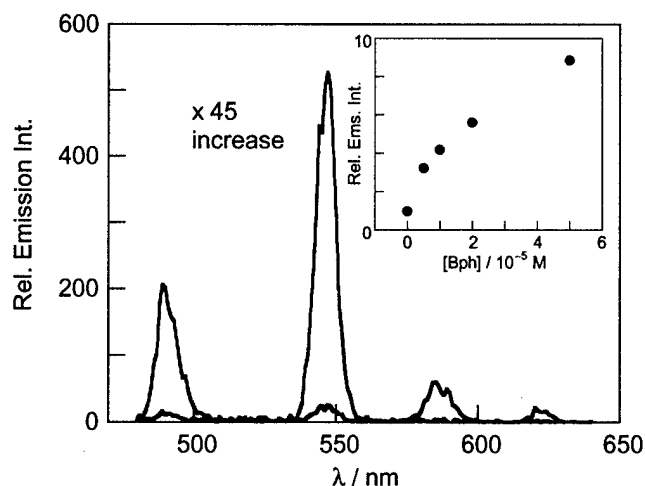
Scheme 4

7
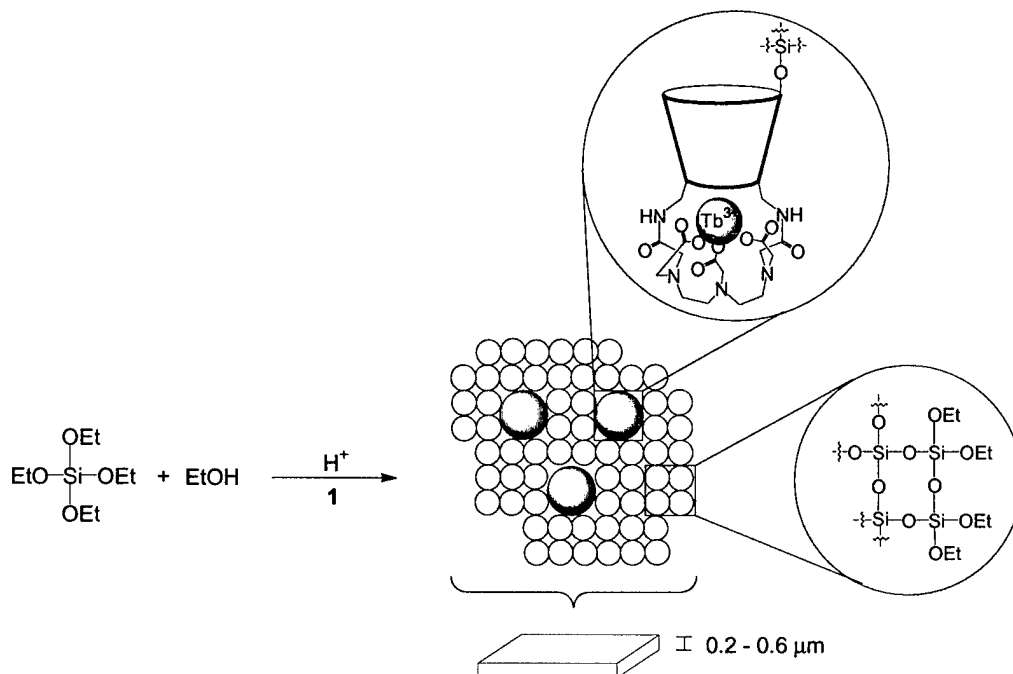
Figure 3. Emission triggered by biphenyl (the x45-fold increase occurs for 50 μM) introduced as an aqueous solution onto films prepared according to Scheme 4.

singlet excited state to the triplet is prompt (2 ns). Subsequent energy transfer from biphenyl to the Tb^{3+} ion occurs in 26 μs whereupon luminescence from the DTPA-bound Tb^{3+} is detected over the ion's natural lifetime. Our ability to prepare a chemosensing film that exhibits a well-defined optical response poises us to undertake the microfluidic experiments proposed in Section 3.2.1.2.

2.2. Pressure Sensing at Aerodynamic Surfaces

Beyond the chemical environment, the Air Force faces challenges in sensing many different types of physical phenomena. The measurement of surface pressures in aerodynamics testing is especially prominent in Air Force efforts to design high performance aircraft. Most surface pressure measurements rely on taps and transducers. These longstanding and conventional methods, however, are inadequate for many applications because they are single point measurements that can be time consuming and expensive. In recent years, Pressure sensitive paints (PSPs) have been developed that allow direct measurement of continuous pressure fields over large surfaces [14]. The basic idea of the PSP approach is to incorporate oxygen quenchable lumophores in air permeable matrices, which may be "painted" onto a surface of interest. Under static conditions, a baseline luminescence is observed from the painted surface - this glowing image may be optically captured, thereby establishing a reference calibration map. Under flow conditions, air is brought to the surface of the paint and the equilibrium concentration of oxygen permeating the matrix will vary with pressure. Because the long-lived phosphorescence is quenched by oxygen, the intensity of the luminescence is attenuated as the concentration of the oxygen within the matrix, and correspondingly the pressure of air at the surface of the matrix, is increased.

Current PSP measurements rely on emission from Pt^{II} porphyrin and Ru^{II} polypyridyl lumophores. The prominence of these lumophores as probes for PSPs is largely historical, building on initial developments in the field. From the perspective of excited state design, they are not, however, optimal lumophores for many pressure measurements, especially for those of current interest to the Air Force. Both types of excited states decay by phonon coupling to high-energy stretching vibrations ($\sim$1,500 cm^{-1}) associated with the organic framework of the ligand (C=C and C=N vibrations). Within the context of nonradiative decay theory, these high-energy vibrations provide an effective thermal sink for nonradiative decay over the critical temperature range of 20 - 100 °C. Consequently, the accuracy of pressure intensity maps is compromised because large variations in the intensity arise from temperature fluctuations during the pressure

8

measurement. For this reason, temperature calibrations of the PSPs commonly require separate wind tunnel runs.

Owing to the enormous expense of running wind tunnel facilities, the Experimental Operations and Diagnostics Branch of the Aeromechanics Division of the Flight Dynamics Directorate at Wright Patterson AFB was interested in eliminating temperature calibration runs in its subsonic wind tunnel facility. In response to this Air Force need, we set out to develop a luminescence "thermometer" that could be incorporated into PSPs currently used by the Air Force. The search for an adequate PSP "thermometer" was performed under the following constraints:

- The temperature probes had to be incorporated into PSP binders with the same preparative conditions used to formulate the paint.

- The luminescence from the temperature probe had to exhibit a negligible dependence on oxygen concentration (i.e., no O_2-based quenching) such that the only change in luminescence was due to temperature.

- The temperature probes had to be excited at the same frequency as the pressure probes. In the subsonic wind tunnel facility at WFAFB, 440-480 nm diode lasers used to excite PSPs.

- Though excitation wavelengths of pressure and temperature probes had to be co-incident, the luminescence signature of temperature probe must be to longer wavelength ($\lambda_{max} > 600$ nm) than that used to map pressure.

- A change of 1% in luminescence intensity per °C over 5-40 °C was the ideal target response desired for a thermometer.

To briefly summarize the results of an intense two-year research effort, several different classes of luminescent compounds and materials were examined as PSP thermometers. These included acetylacetonate (acac) complexes (acac, phenyl, p-nitrophenyl, and FOD) of lanthanide ions ($Ln^{3+} = Eu^{3+}$, Tb^{3+}, Dy^{3+}), Zn^{2+} diphenyl phenanthroline complexes, laser dye impregnated silica spheres and nanocrystalline quantum dots (QDs). In this exhaustive study of potential temperature tracers, we discovered that CdSe QDs met all the above criteria [2.4.6]. Owing to the page constraints of this proposal, we only present details of the QD work.

2.2.1. Nanocrystalline Quantum Dots as Temperature Probes of PSPs

Semiconducting nanocrystallites offer a new type of nanometer size building block for creating novel luminescence-based diagnostics. As a result of the quantum size effect, their electronic states are discrete and tunable with the size of the crystallite (particle-in-a-box) [15-17]. There are now a number of approaches to making nanometer size "boxes" of semiconductors, the most useful of which has been pioneered by our MIT colleague, Moungi Bawendi [18]. CdSe QDs have been synthesized with size distributions smaller than 4%. These nanocrystallites yield a narrow fluorescence band, which can be arbitrarily tuned to any color in the visible, depending on the size of the particle. The CdSe core is typically "overcoated" with a

9

ZnS overlayer, which serves to increase the fluorescence quantum yield. The overcoat has evolved to include a second capping layer consisting of mercapto or phosphite alcohols. This final overcoat layer may be altered to control the solubility of the QDs in polar and non-polar solvents, polymers, and films, including PSP binders. We settled on the CdSe nanocrystallites (depicted in Figure
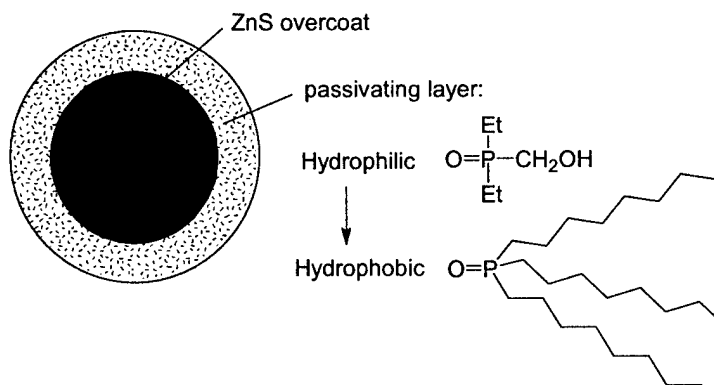

Figure 4. QDs used in PSP studies.

4) possessing a 3-4 monolayer ZnS overcoat and a phosphite alcohol passivating layer, which afforded good solubility in the solvents used to prepare PSP binders.

The CdSe nanocrystals are attractive candidates as temperature probes for PSPs because: (1) Near-Gaussian emission bands possessing narrow widths (FWHM = 30 nm) may be produced across the full range of the visible spectrum (400 nm (15 Å nanocrystals) - 700 (100 Å nanocrystals)) [19]. (2) The photoluminescence quantum yield is high (up to 50% at room temperature). (3) Oxygen cannot diffuse through the solid core of the QD, and therefore the emission is insensitive to oxygen. (4) And the QDs possess a very broad and featureless absorption profile with an extinction coefficient that is essentially invariant from 300 to 480 nm [19]; accordingly, the bright QD emission may be achieved with excitation wavelengths that are co-incident with PSP excitation.

Figure 5 shows the temperature dependence of the emission band for solid films of the phosphite-capped 60-Å CdSe QDs. Spectra were recorded at intervals throughout the temperature range of 5-40 °C. The results are spectacular. The *linear* change in emission intensity of *1.5% per* °C throughout the entire 35 °C range far exceeded Air Force design specifications. The exceptional photostability of the QDs and the reversibility of the luminescence change with temperature is in evidence from the almost perfect superposition of the 25 °C-emission bands of Figure 5 recorded at the beginning, middle, and end of the experiment. As expected, the QDs showed absolutely no dependence on oxygen concentration. Numerous studies were undertaken to assess the generality of

Figure 5. The temperature dependence of the emission profile of CdSe QDs over a 5-40 °C range.

these observations. We found that: (1) The temperature dependence was independent of QD size, allowing us to settle on a QD temperature probe that exhibited emission ($\lambda_{em,max}$ = 600-660 nm) well red of the PSP emission of Ru^{II} polypyridines and Pt^{II} porphyrins. (2) The QD emission properties were independent of the excitation wavelength (consistent with the QD absorption spectrum, which is a broad and intense, extending from the band-edge into the near UV region). This result enabled us to use the output wavelength of the 460-nm diode lasers for pressure and temperature measurements. (3) The appearance of reproducible temperature dependent photoluminescence from QDs in organic and inorganic matrices, as solids and in solution indicated that the effect is related to an internal solid-state process of the QD rather than, for example, a dynamical surface chemical processes. (4) The temperature-dependent photoluminescence response was the same for QDs of low (20%) and high (50%) emission quantum efficiencies. This result showed us that the temperature dependence of the QDs was reliable and did not fluctuate for different sample preparations.

With these results in hand, the QDs were directly passed from the laboratory bench to the Arnold and Wright Labs Directorates for testing and evaluation. This transition was made possible by an STTR involving Innovative Scientific Solutions, Inc. (ISSI), a sub-contractor to the Air Force. All expectations of the QDs as temperature probes were confirmed at Air Force facilities in 6.2 tests carried out by ISSI. It is expected that the QD paints will be commercialized in 6.3 ventures at Arnold and Wright Patterson AFB over the next two years. Contact people and mechanisms are already in place with Air Force Lab directorates. The users of the self-calibrating PSPs will be the Engineering Development Center of Arnold AFB, the Experimental Operations and Diagnostics Branch of the Aeromechanics Division of the Flight Dynamics Directorate (WL/FIMO), and the Test and Evaluation Branch of the Turbine Engine Division and Propulsion and Fuel Combustions Branch of the Fuels and Lubrication Division of the Aero Propulsion and Power Directorate (WL/POTX and WL/POSF, respectively).

2.2.2. Development of High Temperature PSPs

Many other pressure-sensing needs of the Air Force extend beyond current PSP capabilities. One vital area of interest to the Air Force is to obtain pressure maps within jet engines where performance is critically dependent on the pressure field at the surfaces of the compressor and turbine blades. While several Directorates at Air Force labs have prioritized pressure measurements within the compressor and turbine stages, there is no PSP that is stable at the requisite high temperatures (800 - 1000 °C).

Can a high temperature PSP be prepared? We believe so. We are relying on the stability of all-inorganic complexes of the hexanuclear cluster ions, $Mo_6X_8L_6$ and $Re_6Q_8L_6$ (X = halide; Q = S, Se; L = donor ligand). The structures of these clusters consist of an octahedral metal core coordinated by eight-face bridging X or Q ligands and six axial L donor ligands. The clusters exhibit exceptional thermal stabilities, as they are prepared from high temperature liquid melts (600-800 °C). Both hexanuclear molybdenum and rhenium clusters emit with appreciable quantum efficiencies, though the emission wavelength of the molybdenum clusters is in the near-

IR spectral region and consequently difficult to measure with most conventional detectors used in wind tunnels. For this reason, efforts were shifted to investigations of the photophysics of the rhenium clusters, which exhibit a bright emission in the red region of the visible spectrum that is easily detectable by eye, film and conventional detectors.

Excitation of the ligand-to-metal charge transfer (LMCT) transition, which dominates the absorption spectra of $[Re_6Q_8]^{2+}$ clusters in the 210-500 nm region elicits a broad, structureless and intense emission extending from ~600-1000 nm. The room temperature (298 K) luminescence data listed for selected compounds in Table 1 show that some of the clusters are intensely luminescent in the red spectral region with quantum yields as high as 20%. This intense luminescence is efficiently quenched by oxygen according to the same mechanism that we have defined for the molybdenum clusters [*2.4.7* and *2.4.8*]. This result sets the stage for the development of the rhenium clusters as probes for high temperature PSPs.

Our preliminary analyses of the data of Table 1 reveal that the emission properties are largely relegated to the $[Re_6Q_8]^{2+}$ core and that the axial ligands perturb this emission in a minor and understandable way [*2.4.9*]. In the long run, this convenience will allow us to tune the physical and photophysical properties of the clusters for their facile incorporation into high temperature PSP binders (e.g., porous oxides prepared from sol-gels). Of the clusters listed in

Table 1. Excited-State parameters for the hexanuclear rhenium(III) chalcogenide clusters.[a]

Cmpd No.	Clusters[b]	E_{em} (10^3 cm^{-1})	ϕ_{em}[d]	τ_o (μs)
3	$[Re_6S_8Cl_6](Bu_4N)_4$	13.27	0.007	5.1
4	$[Re_6S_8Br_6](Bu_4N)_4$	12.85	0.001	3.9
5	$[Re_6S_8I_6](Bu_4N)_4$[c]	12.50	0.001	2.6
6	$[Re_6S_8(PEt_3)_6]Br_2$	13.90	0.044	10.0
7	$[Re_6Se_8(PEt_3)_6]I_2$	13.70	0.068	10.8
8	$[Re_6Se_8(CH_3CN)_6](SbF_6)_2$[c]	14.40	0.100	14.8
9	$[Re_6Se_8(Pyridine)_6](SbF_6)_2$[c]	14.50	0.163	14.0
10	$[Re_6Se_8(DMF)_6](SbF_6)_2$[c]	14.70	0.203	18.9
11	$[Re_6Se_8(DMSO)_6](SbF_6)_2$[c]	15.10	0.238	22.4
12	*trans*-$Re_6Se_8(PEt_3)_4I_2$	13.40	0.037	5.4
13	*cis*-$Re_6Se_8(PEt_3)_4I_2$	13.30	0.029	6.0
14	$Re_6Se_8(PEt_3)_5I(I)$	13.50	0.085	6.5
15	$Re_6S_8(PEt_3)_5Br(Br)$	13.53	0.043	7.0
16	*trans*-$Re_6S_8(PEt_3)_4Br_2$	13.48	0.008	5.7
17	*cis*-$Re_6S_8(PEt_3)_4Br_2$	13.33	0.010	4.8
18	*mer*-$Re_6S_8(PEt_3)_3Br_3$	13.04	0.019	4.2

[a] E_{em} is the corrected emission energy maximum, ϕ_{em} the quantum yield for emission, and τ_o the observed luminescence lifetime. [b] Parameters measured in deoxygenated CH_2Cl_2 at 23 ± 2 °C unless otherwise noted. [c] Parameters for compounds **5**, **8-11** were measured in neat or excess axial ligand. [d] Error in quantum yield measurements is ±10%; absorbances of all solutions were ≤ 0.1.

Table 1, the phosphine- and chloride-substituted clusters, $[Re_6Se_8(PEt_3)_6]^{2+}$ and $[Re_6S_8Cl_6]^{4-}$, appear to best be suited for PSP applications. As described in Section 3.2.3.1, we will investigate these clusters to acquire a deep understanding of the nonradiative decay pathways of these probes. On the basis of these studies, the emission properties of the clusters at high temperature will be optimized for PSP implementation.

2.3. Sensor Materials for Vorticity Measurements of Highly Turbulent Flows

In addition to pressure sensing, the design of high performance aircraft is aided by the quantitative measurement of highly turbulent flows at aerodynamic surfaces. State-of-the-art optical techniques for measuring fluid flow currently rely on imaging velocity of particles (PIV) [20]. While enormously powerful, the PIV technique is constrained in its application to flows at aerodynamic surfaces because (1) the flow is highly 3-D in character (PIV measures particle motion within a sheet of laser light and thus cannot accommodate out-of-plane motion), (2) particles have their own inertia and they therefore may not faithfully track the flow, especially when it changes suddenly at a surface, and (3) particles do not go into the critical boundary layer of a surface or in areas where turbulence is high - two important regimes in aerodynamic studies. In response to the challenge of providing a quantitative measure of turbulent flows at boundaries, we have invented a new technique called Molecular Tagging Velocimetry (or MTV) [2.4.10 and 2.4.11], which allows us to physically sense flow by precisely describing the velocity profile of a fluid. In the MTV experiment, particles are replaced with optical supramolecular tracers. Since the supramolecules are part of the flow (they are molecularly dissolved within the fluid), all the problems associated with particles are eliminated in the MTV technique. The optical supramolecules are dissolved in the fluid and a grid of laser lines is imposed upon the flow by shining a laser beam off of a grating to produce a glowing grid, defined by the luminescence from the optical supramolecule tracer. The trace must exhibit a bright, non-quenchable luminescence, which is sufficiently long lived to convect with the flow (μs to ms depending on the fluids problem). The deformation of the grid as it moves with the flow is recorded with a CCD camera. By measuring the distance and direction each grid intersection travels and knowing the time delay between each image, the two velocity components in the grid plane may be determined (the out-of-plane velocity can be determined with a second CCD camera). Parameters important to the fluid physicist, such as turbulence intensities, the Reynolds stress and vorticity may be calculated.

The special properties of the MTV technique permit us to investigate many problems of interest to the Air Force that previously were elusive to the fluid physicist. One important problem is the measurement of the velocimetry flow field of a rotating airfoil. With increasing attack angle, turbulence at the front or leading edge of the airfoil causes the flow to detach. This situation results in dynamic stall and the plane looses lift, thereby catastrophically affecting the flight of the aircraft. With less dire consequences, when the smooth or laminar flow over a wing becomes turbulent, the drag increases thereby resulting in losses in flying efficiency. The leading edge problem is uniquely addressed by the MTV technique owing to its high 3-D character and
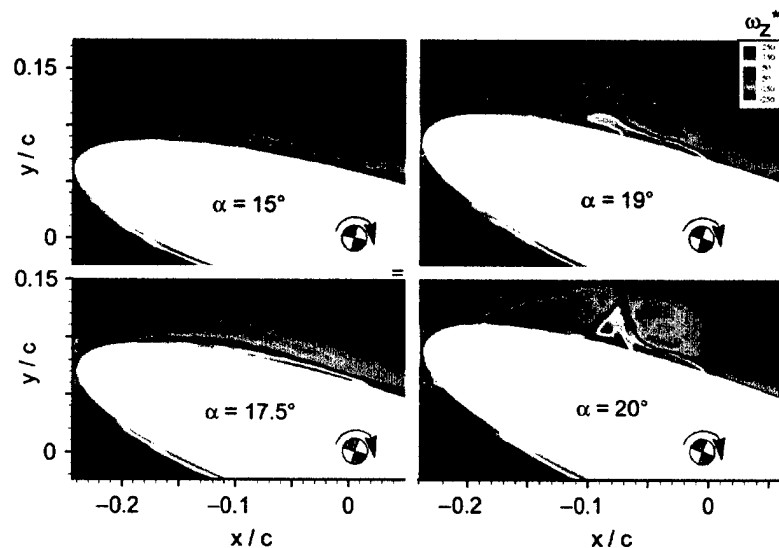
13

Figure 6. Evolution of the vorticity field as measured by MTV at the onset of leading edge separation on an airfoil pitching at high angles of attack. The color scale indicates the *quantitative* magnitude of vorticity. Purple indicates the most intense clockwise flow and red indicates the most intense counterclockwise flow.

large range of spatial and temporal scales. Accordingly, during the past funding period, we implemented the MTV technique in the labs of Dr. M. M. Koochesfahani to experimentally examine the leading edge problem for the AFOSR Engineering Directorate (AFOSR F49620-95-1-0391); Dr. Miguel Visbal of the Aeromechanics Division, Wright Labs Flight Dynamics Directorate, had previouly computationally examined the problem at Wright Patterson Labs.

Figure 6 represents the first detailed picture of a flow within the boundary layer near the surface of a pitching airfoil [2.4.12 and 21]. The color scale indicates the *quantitative* magnitude of vorticity, the fundamental parameter of turbulence; purple, blue and green indicate a clockwise flow and yellow and red indicate a counterclockwise flow. Among the many details resolved in these measurements is the occurrence of a thin flow traveling in the reverse direction near the airfoil surface. It is this reverse flow, creeping backwards up the airfoil that causes the eruption of the boundary layer away from the wing in a highly localized manner (both spatial and temporal). These results point the way toward the design of static and active control features that can minimize the reverse flow, thus providing a road map to the design of safer and higher performance aircraft.

2.4. List of Publications from Previous Grant Cycle

1. "Buckets of Light"; Christina M. Rudzinski and Daniel G. Nocera, *Molecular and Supramolecular Photochemistry*; V. Ramamurthy and K. S. Schanze, Eds.; Marcel-Dekker **2000**, in press.

2. "Lanthanide-Ion Modified Cyclodextrin Supramolecules"; Christina M. Rudzinski, Wanda K. Hartmann and Daniel G. Nocera, *Coord. Chem. Rev.* **1998**, *171*, 115.

3. "Chemosensing of Monocyclic and Bicyclic Aromatic Hydrocarbons by Supramolecular Active Sites"; Wanda K. Hartmann, Mark A. Mortellaro, Zoe Pikramenou and Daniel G. Nocera, *Chemosensors of Ion and Molecule Recognition*; NATO ASI Series, Series C:

Vol. 492; J.-P Desvergne and A. W. Czarnik, Eds; Kluwer Academic; Dordrecht, **1997**; p. 159.

4. "Mechanism for the Sensitized Luminescence of a Lanthanide-Ion Macrocycle Appended to a Cyclodextrin"; Christina M. Rudzinski, Wanda K. Hartmann and Daniel G. Nocera, *J. Phys. Chem.* **1998**, *102*, 7442.

5. "Optimized Detection of Aromatic Hydrocarbons in Aqueous Solution by Lanthanide-Ion Modified Cyclodextrin Supramolecules"; Christina M. Rudzinski, Scott D. Carpenter and Daniel G. Nocera, to be submitted to *J. Am. Chem. Soc.*

6. Patent application, "Quantum Dots as Luminescent Temperature Probes"; Alfred A. Barney, Moungi G. Bawendi, Vikram Chandrasekar Sundar, Daniel G. Nocera, Christina M. Rudzinski and Glen W. Walker, May **2000**.

7. "Fiber Optic Oxygen Sensing via Luminescence from Molybdenum Chloride Clusters," Ruby N. Ghosh, Gregory L. Baker, Cory Ruud and Daniel G. Nocera, *OSA Tech. Digest Ser.* **1997**, *16*, 366.

8. "Fiber Optic Oxygen Sensor using Molybdenum Chloride Cluster Luminescence"; Ruby N. Ghosh, Gregory L. Baker and Cory Ruud and Daniel G. Nocera, *Appl. Phys. Lett.* **1999**, *75*, 2885.

9. "Highly Emissive Hexanuclear Rhenium(III) Clusters $[Re_6S_8]^{2+}$ and $[Re_6Se_8]^{2+}$"; Thomas G. Gray, Christina M. Rudzinski, Daniel G. Nocera and R. H. Holm, *Inorg. Chem.* **1999**, *38*, 5932.

10. "Molecular Tagging Diagnostics for the Study of Kinematics and Mixing in Liquid Phase Flows"; Manoochehr M. Koochesfahani, Richard K. Cohn, Charles P. Gendrich and Daniel G. Nocera, *Developments in Laser Techniques in Fluid Mechanics*, R. J. Adrian, D. F. Durao, F. Durst, M. V. Heitor, M. Maeda, J. Whitelaw, Eds., Springer-Verlag, Berlin, **1997**, p. 125.

11. "Molecular Tagging Velocimetry and other Novel Applications of a New Phosphorescent Supramolecule"; Charles P. Gendrich, Manoochehr M. Koochesfahani and Daniel G. Nocera, *Exp. Fluids* **1997**, *23*, 361.

12. "Molecular Tagging Velocimetry: A Review of Techniques, Chemical Concepts, and Applications"; Manoochehr M. Koochesfahani and Daniel G. Nocera, *Annu. Rev. Fluid Phys.* **2000**, submitted for publication.

13. "Synthesis of an Anionic Tridentate Phosphinoborate and its Reaction Chemistry with Sn(II)"; Alfred A. Barney, Alan F. Heyduk, and Daniel G. Nocera, *Chem. Commun.* **1999**, 2379.

2.5. Literature Citations

1. M. U. Kumke, H.-G. Lohmannsroben and T. Roch, *J. Fluorescence* **1995**, *5*, 139.

2. J. J. Harvath, M. Gueguetchkeri, A. Gupta, D. Penumatchu, H. H. Weetall, In *Biosensor and Chemical Sensor Technology*; K. R. Rogers, A. Mulchandani, W. Zhou, Eds., ACS Symposium Series 613, American Chemical Society, Washington, D.C., **1995**, Ch. 5.

3. A. P. de Silva, H. Q. N. Gunaratne, T. Gunnlaugsson, A. J. M. Huxley, C. P. McCoy, J. T. Rademacher and T. E. Rice, *Chem. Rev.* **1997**, *97*, 1515.

4. (a) *Chemosensors of Ion and Molecular Recognition*, NATO ASI Series C, Vol. 492, J.-P. Desvergne and A. W. Czarnik, Eds., Kluwer Academic, Dordrecht, The Netherlands, **1997**. (b) *Fluorescent Chemosensors for Ion and Molecule Recognition*, ACS Symposium Series 538, A. W. Czarnik, Ed., American Chemical Society, Washington, D.C., 1993. (c) A. W. Czarnik, *Acc. Chem. Res.* **1994**, *27*, 302.

5. H.-J. Schneider, F. Hacket, V. Rudiger and H. Ikeda, *Chem. Rev.* **1998**, *98*, 1765.

6. M. V. Rekharsky and Y. Inoue, *Chem. Rev.* **1998**, *98*, 1875.

7. J. Janata, *Principles of Chemical Sensors*, Plenum Press, New York, **1989**.

8. *Sensors: A Comprehensive Survey. Fundamentals and General Aspects*, Vol. 1., W. Göpel, J. Hesse and J. N. Zemel, Eds., VCH, New York, **1988**.

9. M. A. Mortellaro and D. G. Nocera, *J. Am. Chem. Soc.* **1996**, *118*, 7414.

10 Z. Pikramenou and D. G. Nocera, *Proc. Sixth Int. Symp. Cyclodextrins*, Editions de Santé, Paris, **1993**, 259.

11. F. J. Steemers, W. Verboom, D. N. Reinhoudt, E. B. van der Tol and J. W. Verhoeven, *J. Am. Chem. Soc.* **1995**, *117*, 9408.

12. H. Matsumoto and S. Shinkai, *Chem. Lett.* **1994**, 901.

13. N. Sabbatini, M. Guardigli, A. Mecati, V. Balzani, R. Ungaro, E. Ghidini, A. Casnati and A. Pochini, *J. Chem. Soc. Chem. Commun.* **1990**, 878.

14. B. G. McLachlan, J. L. Kavandi, J. B. Callis, M. Gouterman, E. Green, G. Khalil and D. Burns, *Exp. Fluids* **1993**, *14*, 33.

15. (a) L. E. Brus, *Appl. Phys. A* **1991**, *53*, 465. (b) M. G. Bawendi, M. L. Steigerwald and L. E. Brus, *Annu. Rev. Phys. Chem.* **1990**, *41*, 477.

16. S. A. Empedocles and M. G. Bawendi, *Acc. Chem. Res.* **1999**, *32*, 389.

17. (a) A. P. Alivisatos, *Science* **1996**, *271*, 933. (b) A. P. Alivisatos, *J. Phys. Chem.* **1996**, *100*, 13226.

18. C. B. Murray, D. J. Norris and M. G. Bawendi, *J. Am. Chem. Soc.* **1993**, *115*, 8706.

19. B. O. Dabbousi, J. Rodriguez-Viejo, F. V. Mikulec, J. R. Heine, H. Mattoussi, R. Ober, K. F. Jensen and M. G. Bawendi, *J. Phys. Chem. B* **1997**, *101*, 9463.

20.   R. J. Adrian, *Ann. Rev. Fluid Mech.* **1991**, *23*, 261.

21.   C. P. Gendrich, Ph.D. Thesis, Michigan State University, **1998**.